COBEM 2023 27TH INTERNATIONAL CONGRESS OF MECHANICAL ENGENEERING

ABCM Brazilian Society of Mechanical Sciences and Engineering
27th ABCM International Congress of Mechanical Engineering
December 04-08, 2023, Florianópolis-SC, Brazil

# COB-2023-0399
# ON THE PREDICTION OF CRITICAL HEAT FLUX VIA GENERALIZED ADDITIVE MODELS (GAMS)

**Renan Santos Barbosa**
Aeronautics Institute of Technology
renan.barbosa@ga.ita.br

**Camila de Souza**
University of Western Ontario
camila.souza@uwo.ca

**Guilherme Ribeiro**
Aeronautics Institute of Technology
gbribeiro@ita.br

***Abstract.*** *The critical heat flux is the heat flux value in the boiling or cooling process in which the heat transfer decreases, and the heated surface temperature rises rapidly due to factors such as the presence of vapor films and bubbles. Due to the difficulties in elaborate experiments and disagreements about measurement and evaluation techniques related to CHF, some methods, like lookup tables, physical correlations, and machine learning, try to predict CHF. These methods use experimental variables to estimate the CHF value, like pressure, temperature, and mass flux. Generalized additive models (GAMs) are a type of regression model that extends the applications of generalized linear models (GLMs), giving the possibility to model nonlinear associations between the response variable (CHF) and their predictors. GAMs use smoothing functions to estimate the relations, allowing the GAMs models to be more flexible in modeling nonlinear relationships and control predictive aspects like bias and variance to prevent overfitting. This work presents the results using generalized additive models (GAMs) to predict critical heat flux on water-related data. Moreover, this work evaluates the capability of GAMs models in predicting CHF compared to other methods like the lookup table and machine learning models.*

***Keywords:*** *Critical Heat Flux, Generalized Additive Models, Machine Learning, Lookup Table.*

## 1. INTRODUCTION

The critical heat flux can be interpreted as the critical value in which the boiling heat transfer decreases, leading to a fast rise in the heated surface temperature. A thin insulating vapor layer forms on the heated surface at this critical threshold, inhibiting direct contact between the liquid and the surface. As a result, the wall temperature rises rapidly, leading to potential material damage, reduced efficiency, and the possibility of structural failure as in typical water-cooled reactors (Groeneveld et al., 2007).

Despite many studies on the critical heat flux (Groeneveld et al., 2018), this topic can still be improved and discussed. An accurate estimate of the CHF is crucial in the design and safety assessment of energy systems reliant on high-temperature processes found in thermal power plants, industrial boilers, and aerospace propulsion systems. Understanding and predicting CHF is essential in these applications to prevent catastrophic failures caused by local overheating and subsequent material damage. By accurately estimating the CHF, engineers can optimize heat transfer mechanisms, determine appropriate cooling strategies, and ensure the safe operation of these systems. Thus, predicting CHF enables the identification of operational limits, guides the design of heat exchange surfaces, and assists in selecting appropriate coolant flows, ultimately leading to enhanced efficiency, reliability, and safety of energy systems operating under high-temperature conditions (Groeneveld et al., 2007).

Methods to predict the critical heat flux date back to the ’50s (Groeneveld et al., 2018), and the need for more sophisticated methods arose as nuclear reactors worldwide increased. Hundreds of CHF correlations have been reported (Groeneveld, 2018). From the modeling perspective, these methods can be classified into physical, machine learning, and hybrid models. The physical ones use physical properties and analytical tools to develop CHF correlations. The lookup table from Groeneveld et al. (2007), the proposed equations by Katto (1985), and the correlation proposed by Liu et al. (2000) are examples of the physical methods. Machine learning tools can be used to predict better CHF, like the studies by Rassoulinejad (2021). Hybrid models use the knowledge from physical properties and the prediction capability from machine learning models combined to get better predictive performance than other methods (Zhao et al., 2020).

In this work, we propose using generalized additive models (Hastie and Tibshirani, 1986) to predict CHF. A generalized additive model (GAM) is an extension to statistical linear regression in which the use of smoothing functions on the inputs creates the possibility to capture nonlinear relationships between them and the response CHF. The GAM model can be seen as an intermediate approach between linear regression and black-box methods, giving the possibility of good prediction performance while maintaining interpretability. We evaluate the performance of GAMs in predicting CHF using two datasets, Groeneveld's (Groeneveld, 2019) and Zhao's (Zhao et al., 2020). We compare the prediction results from GAMs to the ones from random forests and Groeneveld's lookup table.

Section 2 describes the types of CHF prediction methods assessed: GAMs, Groeneveld's lookup table, and random forests. Section 3 describes the datasets used to train and validate the model's performance and the necessary data cleaning and adjustment. Section 4 presents the procedure to train the models and the chosen performance metrics. Section 5 shows the results of the trained models and their predictive performance, comparing the GAM model with the other models, and the limitations of GAMs are discussed.

## 2. CHF PREDICTION

### 2.1 Generalized additive models (GAMs)

Generalized additive models (GAMs) are an extension of the generalized linear model (GLM), where in addition to the GLM common characteristics, a sum of smooth functions is added to the model linear predictor, making possible the use of nonlinear relationships between the response variable and its predictors without a parametric specification of these relations. Introduced by Hastie and Tibshirani (1986), the GAM model is formulated in Eq. (1).

$$g\big(\mathrm{E}(\mathrm{Y})\big) = \beta_0 + \mathrm{f}_1(\mathrm{x}_1) + \mathrm{f}_2(\mathrm{x}_2) + \mathrm{f}_3(\mathrm{x}_3) + \cdots + \mathrm{f}_\mathrm{m}(\mathrm{x}_\mathrm{m}), \tag{1}$$

where Y is the CHF, $\mathrm{x_j}$, for j=1, …, m, are the explanatory variables like pressure, diameter, etc., and g is a link function that relates the expected values of Y with its predictors. A distribution from the exponential family for Y needs to be specified like the normal distribution discussed in Section 3.3.

The functions f_1, …, f_m specified in Eq. (1) are smooth functions represented by a linear combination of basis functions such as cubic splines or thin plate splines; that is:

$$\mathrm{f_j}(\mathrm{x}) = \sum_{\mathrm{k}=1}^{\mathrm{k_j}} \beta_{\mathrm{jk}}\, \mathrm{b_{jk}}(\mathrm{x}), \text{ for j=1, ..., m,} \tag{2}$$

in which $k_j$ is the number of basis functions for each $f_j$, $\beta_{jk}$'s are the unknown coefficients of the expansion, and $b_{jk}(x)$'s are the known basis functions evaluated at x. In this work, we consider the cubic splines as basis functions. Replacing Eq. (2) with Eq. (1) makes it more evident that the model is now a GLM. The $\beta_{jk}$'s are estimated by penalized iteratively re-weighted least squares (Wood, 2017), and the amount of smoothness is determined by restricted maximum likelihood (Wood, 2017).

The capability of GAMs to consider nonlinear relationships while still having the simple form of a GLM can be an advantage compared to domain knowledge models like Groeneveld's LUT and machine-learning black-box models such as the random forests.

Although GAMs may offer an approach to model complex relationships, it comes with computational efforts since it is necessary to iteratively estimate the parameters from the models and the smoothness degree of each basis function. Another task that can increase the computational cost of training GAMs models is using tensor products (Wood, 2017) to add variable interactions in the model. The addition of complexity in the model using high-degree basis functions and tensor products may lead to a model that is time and memory-demanding to train. This work will not compare the memory used and time necessary to train the models discussed in this work by the assumption that after the models are trained, the prediction of new values can be made in real time.

### 2.2 Groeneveld's lookup table (LUT)

The Groeneveld's LUT (Groeneveld et al. 2007) is one of the main methods to predict the CHF. The LUT is a dataset normalized to predict CHF on 8mm vertical round tubes. To predict with the LUT, it is necessary to have the observed pressure in kPa, mass flux in $\mathrm{kgm^{-2}s^{-1}}$, and thermodynamic quality ranging from -0.5 to 1. As the table has only a discrete range of values, it is necessary to make a linear interpolation between the variables and the CHF from the LUT to obtain the CHF. For tubes with diameters with different values than 8 mm, it is necessary to do a correction on the predicted CHF, done by Eq. (3):

$$\mathrm{CHF} = \mathrm{CHF_{8mm}} \left(\frac{D_{real}}{8}\right)^{-1/2}, \tag{3}$$

where $\mathrm{CHF}_{8\mathrm{mm}}$ is the critical heat flux value predicted by the table, $D_{real}$ is the diameter from the observed data. For data with different geometries of tubes like the one provided by Zhao et al. (2020), it is suggested to use the heated diameter Dhz to make the factor correction. The LUT performance will be compared with the GAM model as a standard point of quality to be achieved.

### 2.3 Random forests

Introduced by Breiman (2001), the random forests model uses the concept of ensemble models, where multiple models are combined to get a better response in the prediction process. The random forests combine multiple decision trees, each using a different set of variables and data to be trained. At the final of the training process, each tree will have an output that will be averaged to give the final value for the predicted CHF. This model will be used as a comparison to the GAM model from the machine learning perspective, as this model does not need lots of work to achieve good results.

## 3. DATA

This work uses two sources of data: one is a collection of critical heat flux on water-related data that Groeneveld (2019) used to develop his LUT, and the other is a collection made by Zhao et al. (2020) that comprises different works related to the departure from nucleate boiling. The dataset provided by Groeneveld has been used to develop the models presented in this work, while the data from Zhao will be used to test the prediction quality of the models.

### 3.1 Groeneveld's dataset

This dataset contains roughly 25,000 observations and eight variables. Part of the data comes from a confidential source, so removing these values is necessary. Moreover, the author suggests the removal of some range of values that do not satisfy the following criteria: $3 < D < 25$ mm, L/D ratio ($L/D > 50$ for $x > 0$, $L/D > 25$ for $x < 0$), $100 \leq P \leq 21{,}000$ kPa, $0 \leq G \leq 8{,}000$ $\mathrm{kgm^{-2}s^{-1}}$, and $x < 1.0$, a summary of the data used to train the models after the filter of acceptable values and are shown in Table 1.

Table 1. Summary of Groeneveld's dataset after filtering.

| VARIABLE | SYMBOL | UNIT | MIN | MAX | MEAN | STD |
|---|---|---|---|---|---|---|
| Diameter | D | m | 0.003 | 0.016 | 0.008 | 0.002 |
| Heated length | L | m | 0.18 | 20 | 2.64 | 2.044 |
| Pressure | P | kPa | 100 | 20,000 | 2.649 | 5,570.319 |
| Mass flux | G | $\mathrm{kgm^{-2}s^{-1}}$ | 17 | 7,964 | 2,013 | 1,506.477 |
| Vapor quality | x | - | -0.497 | 0.999 | 0.355 | 0.271 |
| Critical heat flux | CHF | $\mathrm{kWm^{-2}}$ | 50 | 14,760 | 1,785 | 1,535.559 |

The necessary filter reduced the data to 24,335 observations. The distribution of the variables and the relation between them is shown in Figure 1 below, where the full range of values is not available for some variables. The absence of values can make the model have inferior prediction performance compared to areas where the data is dense.

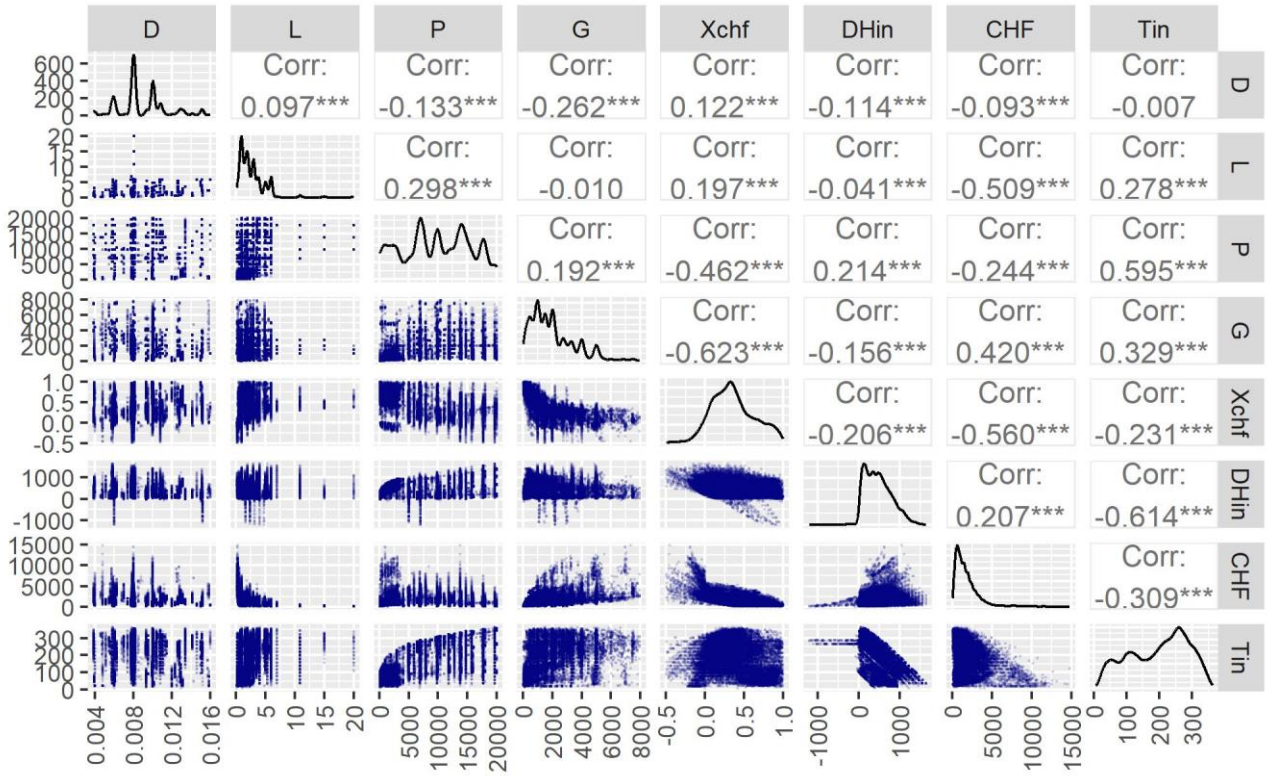


Figure 1. Distribution of Groeneveld's (2019) dataset, on the lower diagonal, a scatterplot of two variables is shown, the diagonal shows the density plot of one variable, and the upper diagonal presents Pearson's correlation between two variables.

### 3.2 Zhao's dataset

The data collected by Zhao et al. (2020) aims to predict CHF in a specific category of the problem named departure from nucleate boiling (DNB), which can be related to working parameters in a nuclear power plant. Because of these specific characteristics, this dataset will test models' prediction capability in a different domain.

This dataset contains 1865 observations and seven continuous variables. Table 2 summarizes the variables, and Figure 2 presents the data distribution.

The evaluation of Zhao's dataset needs to be done cautiously since some range of values of this dataset is out of the available data on Groeneveld's dataset. The extrapolation capabilities of the models will not be evaluated in this work. Zhao's dataset will have its values filtered to be in the same range as Groeneveld's data, resulting in a dataset with 1235 observations.

Table 2. Summary of Zhao's dataset.

| VARIABLE | SYMBOL | UNIT | MIN | MAX | MEAN | STD |
|---|---|---|---|---|---|---|
| Pressure | Pz | MPa | 0.1 | 20.68 | 10.01 | 4.282 |
| Mass flux | Gz | $kgm^{-2}s^{-1}$ | 0 | 7,975 | 2,863 | 1,656.412 |
| Vapor Quality | xz | - | -0.86 | 0.232 | 0.016 | 0.117 |
| Heated diameter | Dhz | mm | 1 | 120 | 16.17 | 21.182 |
| Heated length | Lz | mm | 10 | 3,048 | 911.3 | 726.719 |
| Critical heat flux | CHFz | $MWm^{-2}$ | 0.8 | 19.3 | 3.855 | 1.985 |

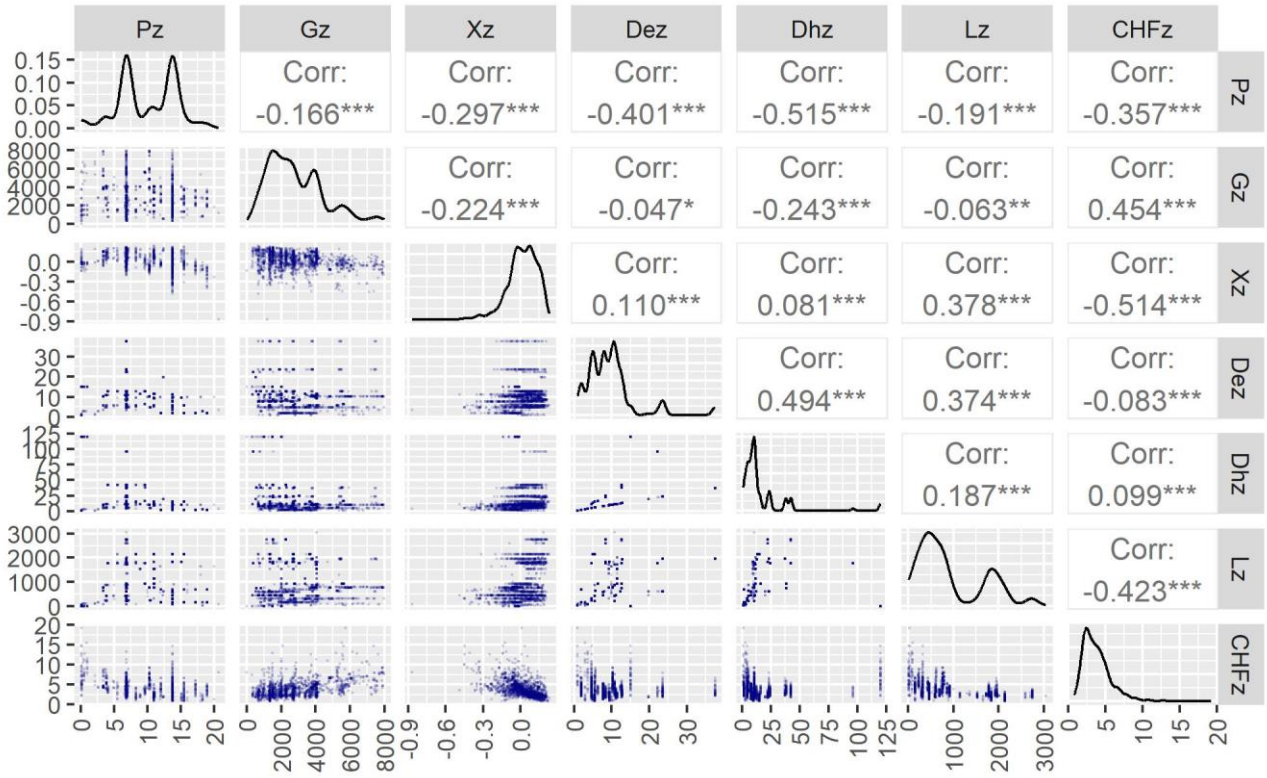


Figure 2. Distribution of Zhao's dataset, on the lower diagonal, a scatterplot of two variables is shown, the diagonal shows the density plot of one variable, and the upper diagonal presents Pearson's correlation between two variables.

### 3.3 CHF distribution

Since the generalized additive model is an extension of the statistical linear model, a good definition of the probability distribution of the response variable can lead to better results and avoid misleading interpretations of the model predictions. The normal distribution is the first option when adjusting a regression model, but evaluating if this distribution is the most suitable for the data is necessary.

Figure 3 shows the distribution of the CHF on both Groeneveld's and Zhao's datasets in the left panel, where it is possible to analyze that the CHF is a positively skewed distribution, indicating that for these datasets, it is more likely to have low values of CHF than higher ones.

In addition, in the qqplot on the left side, the values are not around the continuous line, indicating that our data does not follow a normal distribution. Furthermore, since our data is positively skewed with observed data only on the $\mathbb{R}^+$, the normal distribution is not the best-suited choice. Applying the log in the response variable allows us to transform our data and approximate it to a normal distribution.

The distribution of the log of the CHF and its qqplot is on the right side of Figure 3 for both datasets. After the transformation, it is possible to suppose that the log of the CHF is a better option to use in the GAM model. However, the exponential of the predicted values must be applied to correct the predictions made by a model with the log transformation.

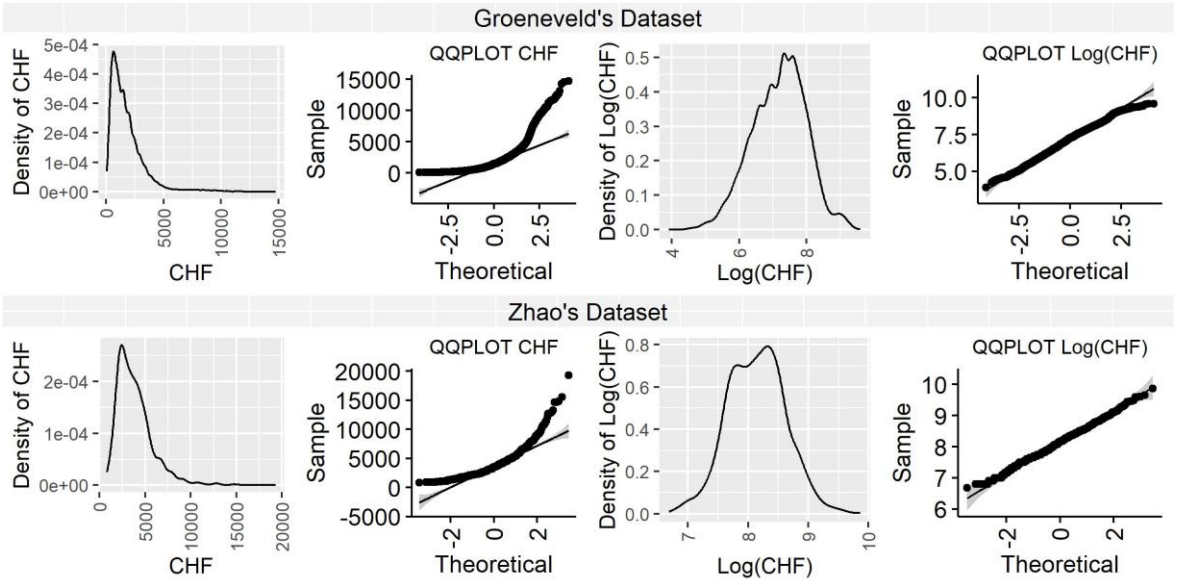


Figure 3. Distribution of Groeneveld's and Zhao's CHF and Log (CHF), the left side shows the density plot and the qqplot of the CHF. On the right side are shown the plots after the log transformation of the CHF.

## 4. MODEL TRAINING AND EVALUATION

Groeneveld's dataset will be used to train and test the GAM and random forests models. Two independent subsamples of the complete data were used: the training dataset with 90% of the data (21901 observations) and the test dataset with the others 10% (2434 observations). Zhao's dataset will be used as validation data, where all the models discussed will be evaluated. This procedure is done to avoid data leakage on the model training and not give benefit to any method.

The root mean squared error (RMSE) shown in Eq. (4) and the percentage of the relative error of the i-observation ($RE_i$) in Eq. (5) will be used to evaluate the model's prediction performance.

$$\mathrm{RMSE} = \sqrt{\frac{1}{n}\sum_{i=1}^{n}(y_i - \hat{y}_i)^2}\,, \tag{4}$$

$$\mathrm{RE_i}\% = \frac{(y_i - \hat{y}_i)}{y_i}\mathrm{x}100, \tag{5}$$

where $y_i$ are the actual CHF values, $\hat{y}_i$ are the predicted values from the model, and $n$ is the number of observations, as any metric can have downfalls in some range of values, plots of the models will be presented to have a better understanding of the model performance.

## 5. RESULTS

This section will show the results of the models discussed in this work. In the first part, a comparison of the model's predictive performance will be calculated, indicating that the GAM model can get similar results compared to the lookup table and the random forests model. In Subsection 5.2, a deeper look at the GAM model results will be presented in detail.

### 5.1 Models comparison

In Table 3, the rmse from the test dataset and Zhao's data were calculated to assess the predictive performance. Figure 4 shows a scatter plot of the observed CHF versus the predicted CHF by the models on both datasets.

The random forests model's performance calculated on the test dataset has the best RMSE. The lookup table has the best RMSE on the filtered Zhao's dataset.

Table 3. RMSE performance comparison.

| Model | Test Dataset | Zhao's Dataset |
|---|---|---|
| Lookup Table | 381.47 | 579.43 |

| | | |
|---|---|---|
| GAM | 293.11 | 669.73 |
| Random Forests | 232.26 | 854.22 |

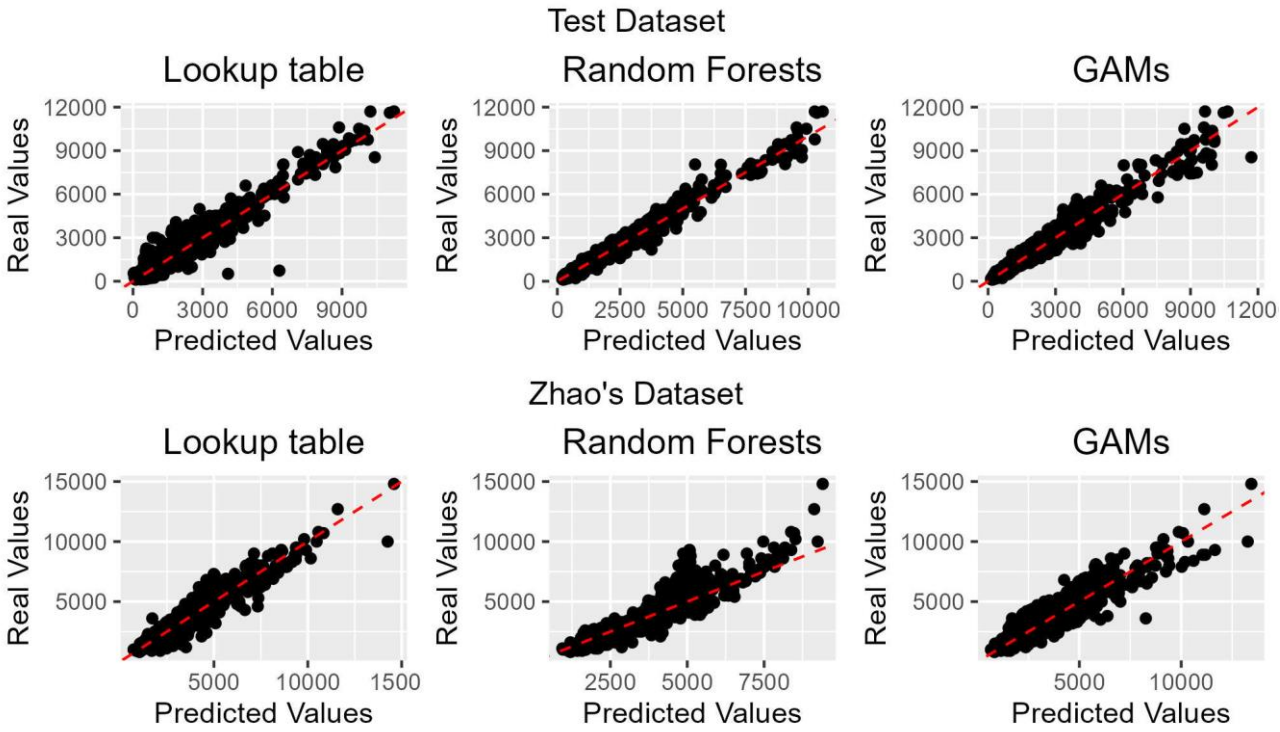


Figure 4. Scatter plot of observed CHF against predicted values from the models adjusted on the test dataset and Zhao's data to access prediction performance.

Another way to access the model's predictive performance is by the percentage of observations with $RE_i$% in a determined bandwidth of relative errors. Table 4 shows the percentage of observations with $RE_i$% between ±20% on both datasets.

Table 4. Percentage of observations with $RE_i$% between ±20%.

| **Model** | **Test Dataset** | **Zhao's Dataset** |
|---|---|---|
| Lookup Table | 70.58% | 85.74% |
| GAM | 84.55% | 75.51% |
| Random Forests | 85.20% | 72.55% |

On the test dataset, the random forests model got the best results. On the other hand, the lookup table got better results on Zhao's dataset, indicating a possible overfitted model trained by the random forests algorithm. Despite not being the best model, the GAM got results close to the other models, with an RMSE 23% smaller on the test dataset than the lookup table but 15% greater on Zhao's dataset. Compared to the random forests model, the GAM model obtained a 21% smaller RMSE on Zhao's dataset even with an RMSE 26% greater on the test dataset, making it a good alternative to predict the CHF by its competitive results, interpretability and more stable predictions on both datasets.

### 5.2 GAMs in depth

As mentioned before, the GAM model can be seen as a GLM. The mgcv package (Wood, 2017) in the R programming language reports the characteristics of the adjusted model. In Table 5, the smoothness of the variables and the interactions given by the tensor product (Wood, 2017) is in the effective degrees of freedom (EDF) column, and the p-value column shows the statistical significance of the variables where values below 0.05 indicate a smooth function that is statistically significant to the model.

Table 5. GAM variable's smoothness complexity and the statistical significance, the term te() indicates a tensor product function of two variables.

| Variable | EDF | P-Value |
|---|---|---|
| P | 21.546 | <2e-16 |
| G | 43.143 | <2e-16 |
| x | 13.220 | <2e-16 |
| D | 38.359 | <2e-16 |
| L | 39.650 | <2e-16 |
| te(P, G) | 14.691 | <2e-16 |
| te(P, x) | 15.285 | <2e-16 |
| te(P, D) | 13.607 | <2e-16 |
| te(P, L) | 14.182 | <2e-16 |
| te(G, x) | 14.006 | <2e-16 |
| te(G, D) | 12.830 | <2e-16 |
| te(G, L) | 13.103 | <2e-16 |
| te(x, D) | 11.178 | <2e-16 |
| te(D, L) | 8.478 | <2e-16 |

Table 5 indicates that the mass flux, diameter, and heated length are the variables with higher smoothness values. All the variables are considered significant by the model trained. Each smoothing function is based on a cubic spline with its own estimated coefficients.

In Figure 5, the smoothing functions of each variable are shown with its 95% confidence intervals, where bigger intervals represent uncertainty areas in which the data is less frequent.

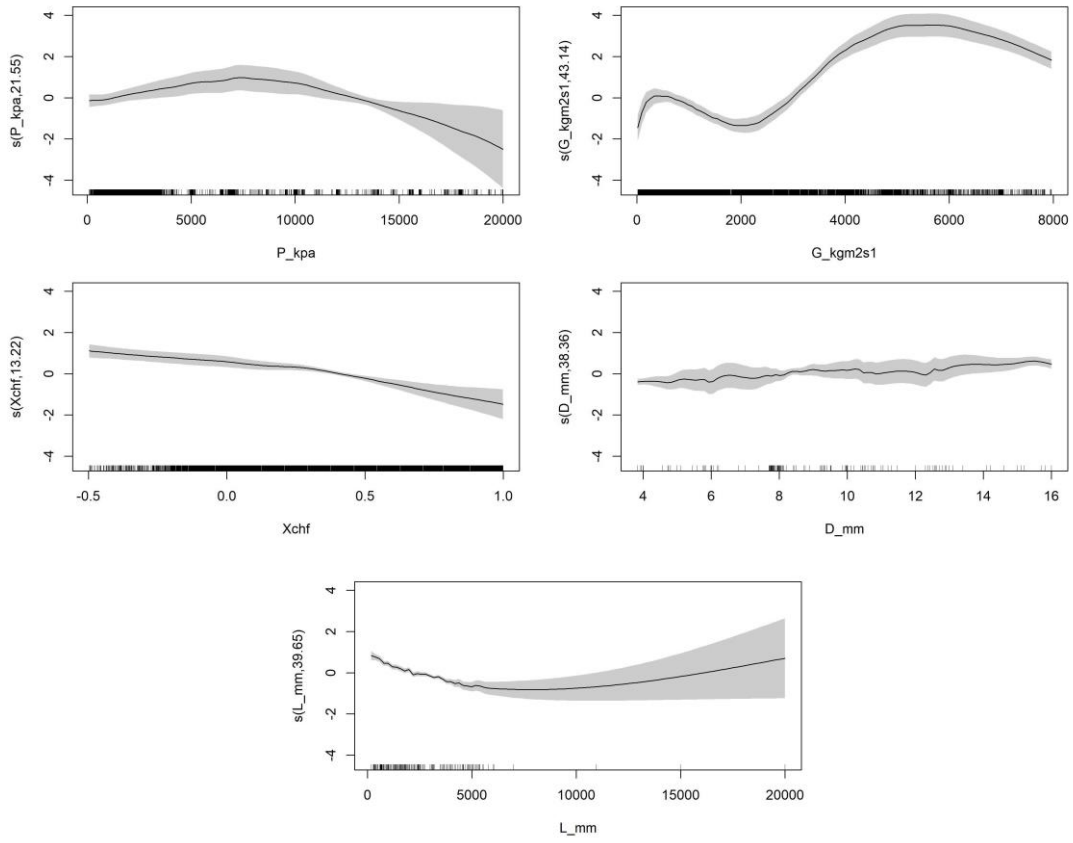


Figure 5. Smoothing functions of the individuals' variables and their 95% confidence intervals, the lines on the x-axis indicate values where data points were observed.

In Figure 6, the contour maps of the smoothing tensor products are shown, where the yellow color indicates the high value of the predicted smooth function, and the red color indicates the low value. The blank areas in the contour plot represent regions in which predictive extrapolation is not recommended. To obtain these areas for each plot a grid of points from the minimum to maximum values of the variables is compared to the observed data by calculating the Euclidean distance. Before calculating the distances, the data and the grid of values are scaled into the unit square. If the Euclidean distance between a pair of points from the grid is greater than 0.1, the pair of values from the grid is not plotted.

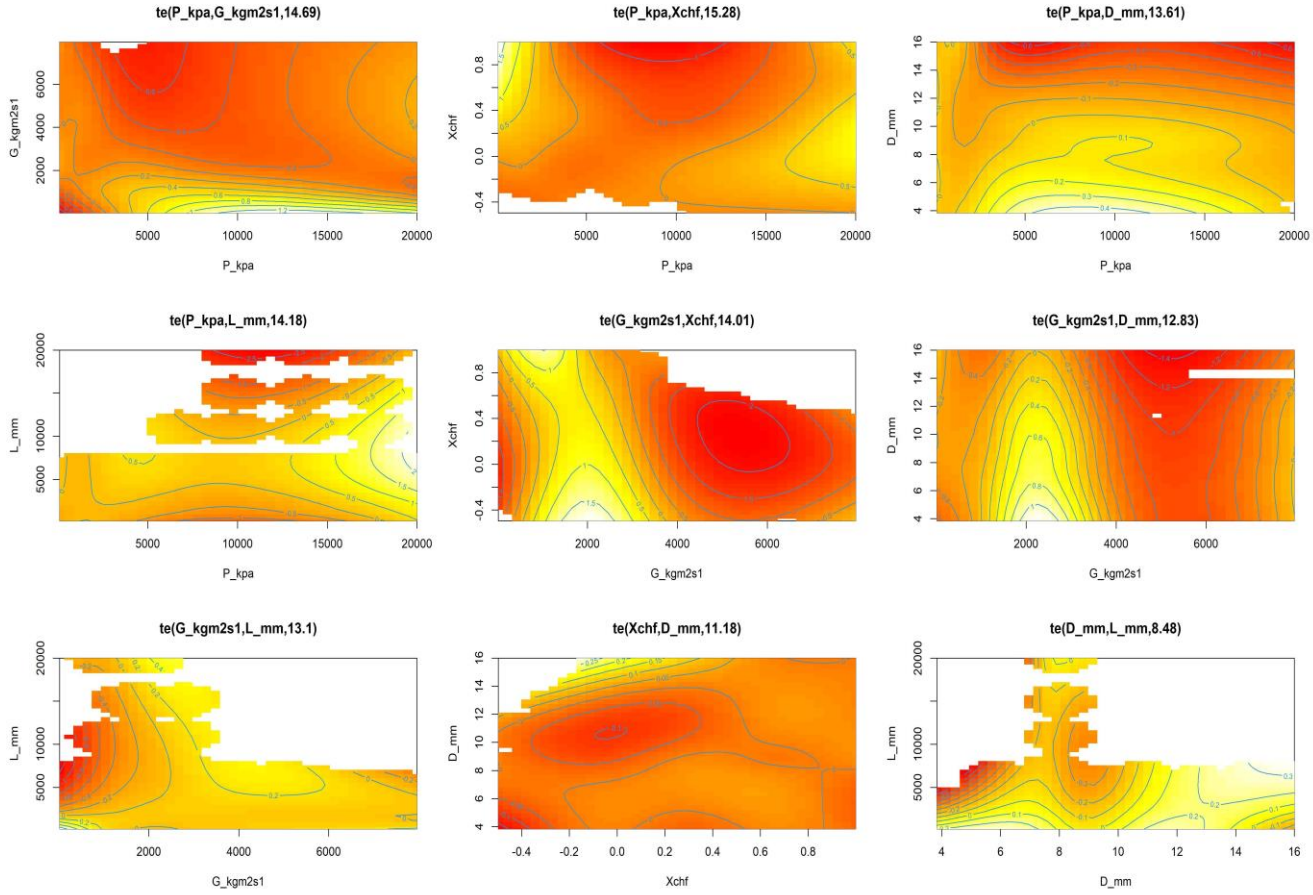


Figure 6. Contour plot of the tensor product smoothed function.

With the information given in Table 5 and Figures 5 and 6, an analyst can better understand the fitted model's behavior and the model's limitations regarding prediction.

## 6. CONCLUSIONS

The results in this work present the generalized additive model (GAM) and how it can be applied to make predictions on the critical heat flux problem, comparing its results with two other models, Groeneveld's LUT and random forests.

Two datasets were used to train and evaluate the proposed models: Groeneveld's (2019) and Zhao et al. (2020). Groeneveld's dataset was separated into two subsamples, one to train the models and the other to test the models' performance. Zhao's dataset was used to validate the models' predictions. To evaluate the models' predictive performance, two metrics were considered: the root mean squared error and the relative error in percentage, where lower values indicate better predictions.

The results show that despite the GAM not being the best model regarding predictive performance, GAM achieved close results compared to the others with RMSE of 293,11 and 669,73 on the test and Zhao's datasets, respectively. These RMSE obtained from the GAM model were 23% smaller than the lookup table on the test dataset and 21% smaller than the random forests model on Zhao's dataset. The GAM model also had 84% and 75% of their relative error measured between ±20%.

In addition to the prediction evaluation, a deeper look at the GAM model was provided. The calculated p-value of the variables indicates that all the terms in the model trained can be considered important to understand the CHF relations.

Figures 5 and 6 indicate that prediction is not recommended on high values of heated length (L) and lower values of vapor quality (x) and pressure (P).

The problem of CHF prediction cannot be seen as a simple predictive problem where only a good prediction tool is enough. Applications that use CHF predictions need a complete understanding of the model behavior to ensure safe operation values on energy systems and when this model is not recommended to be used. From this point of view, GAMs can be an alternative to other predictive techniques since GAMs search for a balance between good predictions (as the lower RMSE on the test dataset in comparison with the lookup table) and interpretability. The interpretation of a fitted GAM model allows analysts to know if a variable or interaction is important to the CHF prediction. Using confidence intervals and contour plots, they can also assess which operation values the predicted CHF are reliable enough to use. These are important features that black-box models like random forests cannot address.

This work is one of the first studies using GAMs in CHF prediction. However, it is still necessary to investigate alternative ways to train this type of model by considering other types of basis functions, new variables, and datasets. Another type of GAM model that can be used is the QGAM, a quantile version of GAM that does not seek the prediction of the expected values like GAMs but a desired quantile to be studied, for example, the 95% quantile of the CHF for an energy system. This approach can be used to develop safety limits and understand which operational values are necessary to obtain this quantile.

## 7. ACKNOWLEDGEMENTS

This study was financed in part by the Coordenação de Aperfeiçoamento de Pessoal de Nível Superior - Brazil (CAPES) - Finance Code 001.

## 8. REFERENCES

Breiman, L., 2001. “Random Forests.” Machine Learning, Vol. 45, pp. 5–32.

Groeneveld, D.C., et al., 2007. “The 2006 chf look-up table.” Nuclear Engineering and Design, Vol. 237, pp. 1909-1922.

Groeneveld, D.C., et al., 2018. “An overview of measurements, data compilations and prediction methods for the critical heat flux in water-cooled tubes.” Nuclear Engineering and Design, Vol. 331, pp. 211-221.

Groeneveld, D.C., 2019. “Critical Heat Flux Data Used to Generate the 2006 Groeneveld Lookup Tables.” Tech. rep., United States Nuclear Regulatory Commission.

Hastie, Trevor and Tibshirani, Robert, 1986. “Generalized Additive Models.” Statistical Science, Vol. 1, pp. 297–318.

Helmryd Grosfilley, Emil, 2022. "Investigation of Machine Learning Regression Techniques to Predict Critical Heat Flux." Master’s thesis, Master Program in Engineering Physics. Uppsala University. Sweden.

Katto, Y., 1985. “Critical heat flux.” Advances in Heat Transfer, Vol. 17, pp. 1–64.

Liu, Wei, et al., 2000. “Prediction of critical heat flux for subcooled flow boiling.” International Journal of Heat and Mass Transfer, Vol. 43, pp. 3371–3390.

Rassoulinejad-Mousavi, Seyed Moein, et al., 2021 "Deep learning strategies for critical heat flux detection in pool boiling." Applied Thermal Engineering, Vol. 190, pp. 116849.

Wood, Simon N., 2017. “Generalized additive models: an introduction with R.” 2nd Edition, Chapman and Hall/CRC.

Zhao, Xingang, et al., 2020. "On the prediction of critical heat flux using a physics-informed machine learning-aided framework." Applied Thermal Engineering, Vol.164, pp. 114540.

## 9. RESPONSIBILITY NOTICE

The authors are the only ones responsible for the printed material included in this paper.